Shape-Dependent Confinement of the Nanodiamond Band Gap

ARTICLE *in* CRYSTAL GROWTH & DESIGN · NOVEMBER 2009

Impact Factor: 4.89 · DOI: 10.1021/cg900680e

1 AUTHOR:

Amanda S Barnard
The Commonwealth Scientific and Industrial…

180 PUBLICATIONS **4,307** CITATIONS

SEE PROFILE

DOI: 10.1021/cg900680e

CRYSTAL GROWTH & DESIGN Article

2009, Vol. 9
4860–4863

Shape-Dependent Confinement of the Nanodiamond Band Gap

Amanda S. Barnard*

CSIRO Materials Science & Engineering, Clayton, Victoria, Australia

Received June 18, 2009; Revised Manuscript Received July 20, 2009

ABSTRACT: By exploiting the link between form and function, the engineering of crystalline materials is providing new opportunities for the development of designer materials, especially at the nanoscale. Tailoring of the nanodiamond band gap remains one of the unresolved challenges in the development of nanodiamond-based electronics, though exceptional progress has been made in controlling particle size and surface properties. In this article electronic structure simulations are used to show that, due to the inhomogeneous distribution of states with respect to the surface, the shape of individual diamond nanocrystals may also offer a way of tuning the band gap within the quantum confinement regime.

Introduction

In recent years, we have seen great progress in the development of designer materials, tailored for a particular purpose through intelligent materials engineering. Crystalline materials are of particular interest, as the symmetry and lattice of the material provides a fundamental template upon which functional shapes can be developed. In particular, this has led to some great successes in controlling the size, shape, and crystal structure (polymorph) of a range of nanomaterials, where the link between form and function is most prevalent. One of the objectives of nanotechnologists is to engineer individual components with atomic level precision, for use in the next generation of electronic devices. In particular, the well documented thermal, mechanical, and electronic properties of the nanocrystalline diamond, along with its chemical compatibility with other types of nanomaterials, make this material an attractive prospect for a variety of applications.[1] Therefore, the electronic properties of isolated diamond nanomaterials[2] and nanocrystalline diamond films[3,4] with grain sizes on the order of ~5−50 nm are receiving considerable attention.

The ability to tailor the properties so as to optimize performance requires a detailed understanding of the relationship between the electronic structure and the materials structure. In the case of nanocrystalline diamond, there has already been some evidence to suggest that tailoring of the electronic properties may be possible, particularly when the particles are within the quantum confinement regime.[5] For example, it has been demonstrated that the hydrogen terminated diamond surfaces and nanoparticles exhibit negative electron affinity (NEA),[6,7] suggesting potential applications in highly efficient solar blind photocathodes and for cold cathode emitters,[8,9] but it is unclear at this stage if this property is amenable to engineering via texturing or control of grain sizes.

Recent density functional theory (DFT) simulations have shown that the electronic orbitals in nanoscale diamond are not homogeneously distributed within individual particles or grains. When dehydrogenated (clean), the core−shell bucky-diamond structure gives rise to different spatial distribution of electronic states, particularly in the vicinity of the interface between the diamond-like core and the fullerenic outer shell.[10,11] Although in excellent agreement with experiment,[10] this is not particularly useful, since the band gap is filled with states from the graphitic component.[11]

In the case of H-terminated nanodiamonds, it has already been demonstrated that the highest occupied molecular orbital (HOMO) at the top of the valence band is dominated by the contribution from carbon atoms in the core, whereas the lowest unoccupied molecular orbital (LUMO) at the base of the conduction band is located on or near the surfaces.[7] This suggests that modifications of the nanomorphology would engineer the HOMO−LUMO band gap,[12] but the structures included in these DFT studies were much smaller than those observed experimentally. To explore this issue more fully, and the possibility of engineering the band gap or NEA, it is necessary to treat a larger set of structures that sample a range of possible shapes and spans the entire quantum confinement regime.

Methods

In the present study we use the density functional based tight-binding method with self-consistent charges (SCC-DFTB),[13,14] which is a two-center approach to DFT, where the Kohn−Sham density functional is expanded to second order around a reference electron density. In this approach, the reference density is obtained from self-consistent density functional calculations of weakly confined neutral atoms, and the confinement potential is optimized to anticipate the charge density and effective potential in molecules and solids. A minimal valence basis is established and one- and two-center tight-binding matrix elements are explicitly calculated within DFT. A universal short-range repulsive potential accounts for double counting terms in the Coulomb and exchange-correlation contributions, as well as the internuclear repulsion, and self-consistency is included at the level of Mulliken charges, as described in ref 14. This method has been selected for use here, as it has previously been shown to be suitable for studying the surface structure and crystallinity of diamond nanoparticles[15,16] and is more computationally efficient than DFT when such a large number of individual calculations are required.

To determine if shape-dependent trends in the electronic properties of diamond nanoparticles exist, it is necessary to individually test a relatively large set of model structures over a range of sizes and shapes. In the present study, 17 particles

*Phone: +61-3-9545-7958. Fax: +61-3-9545-2059. E-mail: amanda.barnard@csiro.au.

 Published on Web 08/04/2009

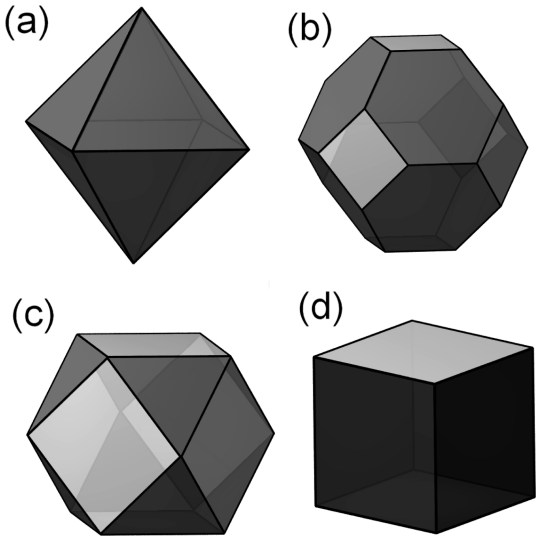

Figure 1. Schematic representations of the (a) octahedral, (b) truncated octahedral, (c) cuboctahedral, and (d) cuboid shapes included in this study.

have been chosen, ranging in size from 259 C atoms (~1.2 nm) to 1798 C atoms (~3.3 nm). Four different shapes have been included, to facilitate the description of shapes enclosed with entirely (111) facets, majority (111) facets, majority (100) facets, and majority (110) facets, as shown in parts a, b, c, and d, respectively, of Figure 1. All test structures were fully relaxed with the conjugate gradient scheme to minimize the total energy (using a 5 meV/Å force convergence), prior to the calculation of the electronic properties.

Note that only two cuboctahedral particles (with majority (100) facets) are included in this study. This is due to morphological ambiguities introduced when cutting along the crystal planes required to achieve this shape. Small structures of this shape were found to have variable degrees of (100)/(111) facet area and could not be unambiguously classed as cuboctahedral (nor truncated octahedral, but something in between). In the present study, care has been taken to ensure that each structure set strictly adhered to the geometric standards of the shape, thereby allowing for reliable trends to be asserted. Alternative shapes may also be explored in future work.

Discussion of Results

In each case the energy was calculated for the Fermi level (E_f), the HOMO, and the LUMO, and is presented in parts a, b, and c, respectively, of Figure 2. Overall, these results show a considerable spread in the values of E_f and the LUMO at small sizes. The variations in the energy of the Fermi level is of particular interest, since aligning this value with other electronic materials is important in designing new devices.[17] However, if we examine the results for individual shapes, defined by the prevalence of particular crystallographic facets, we find the energy of the Fermi level is independent of size in the case of octahedral nanodiamonds but increases within increasing size for all other shapes. The change in energy of the LUMO of octahedral and cuboid shapes is inversely proportional to size, whereas shapes containing a combination of (111) and (100) facets show a different trend. It is interesting to note that the common features among the octahedral and cuboid shapes are the 90° edges and the acute

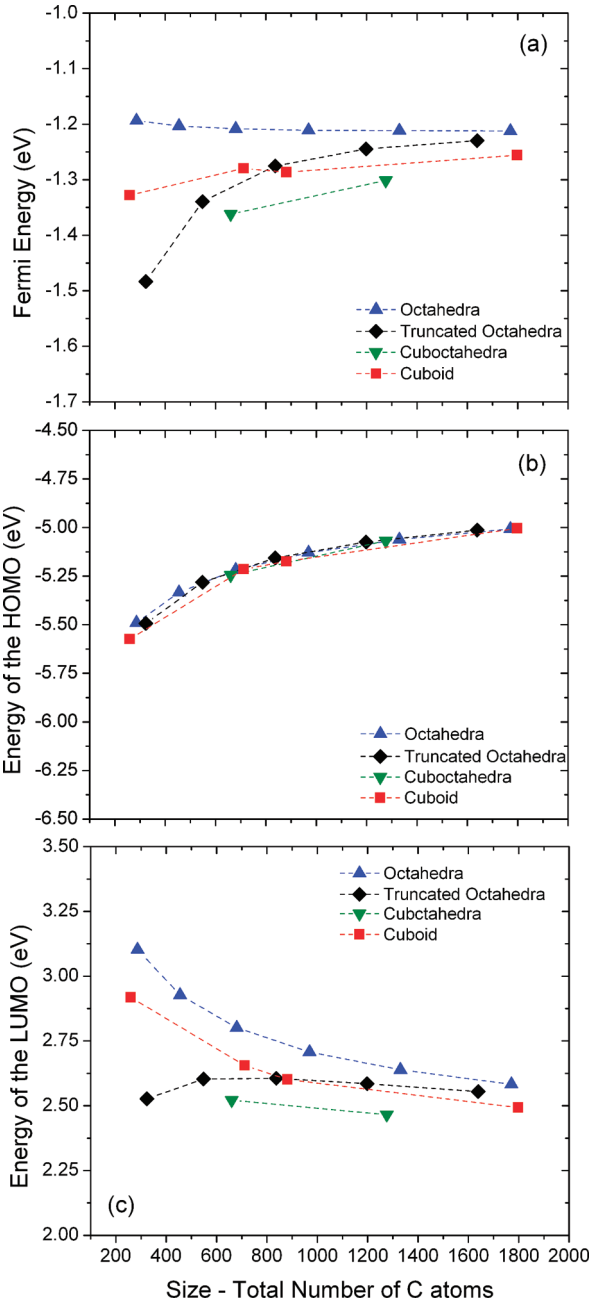

Figure 2. Calculated values of the energy at the (a) Fermi level, (b) HOMO, and (c) LUMO for all of the octahedral, truncated octahedral, cuboctahedral, and cuboid nanodiamonds, as a function of the total number of carbon atoms. Lines are provided to guide the eyes.

corners. It is possible that these geometric features, decorated by highly undercoordinated atoms, may be responsible for this difference, but further work is required to confirm this.

In contrast, the energy of the HOMO is entirely independent of shape, and the results display the characteristic dependence on size that has been demonstrated for small particles using higher level simulations.[7] This indicates that the only way of engineering the HOMO will be to exercise precise control over the particle or grain size and that the introduction of different crystalline facets (via texturing) will not alter the energy of this state.

While the total number of atoms is commonly used as a measure of size, to better relate these trends to the particle

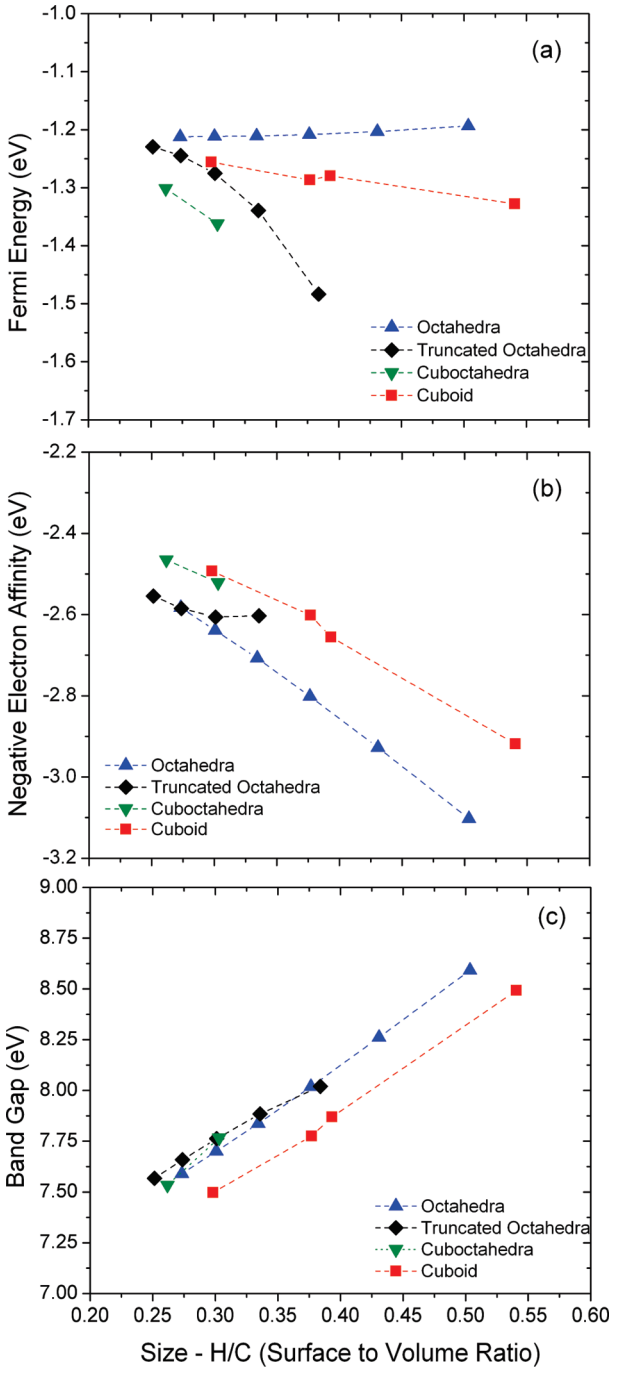

Figure 3. Calculated values of the (a) E_f, (b) NEA, and (c) E_g for all of the octahedral, truncated octahedral, cuboctahedral, and cuboid nanodiamonds, as a function of the surface-to-volume ratio. Lines are provided to guide the eyes.

shapes, the results are recast in terms of the surface-to-volume ratio, which is more descriptive of both the size and shape of nanoparticles. From this perspective, the different trends for each shape are more apparent.

The results in Figure 2 have been used to calculate some further electronic properties in Figure 3, including the HOMO−LUMO band gap and the negative electron affinity. Although it does not change with the nanocrystal shape, if we assume a transition from valence band maximum, we can use the results for the HOMO to obtain an estimate of the NEA,[18] where the influence of shape is observed. These results indicated that the NEA is size-dependent, converging to the bulk value at ~33 nm, and may be engineered by texturing. Similarly, the energy of the Fermi level is also shown to be highly shape dependent, so that the engineering of particular shapes (or facet termination) may improve the alignment of the Fermi levels at interfaces or allow for the tuning to match with ligands or functional groups at the surface.

In the case of the band gap, we see that the shapes enclosed by (111) and (100) facets are all consistent, but the cuboid shape (dominated by (110) facets) exhibits a red-shift in the band gap of ~0.25 eV. While it is known that the band gap may be engineered by controlling the size, this can be difficult to achieve on the industrial scale. The results here indicate that band gap engineering could also be achieved via texturing and the introduction of {110} facets, which may offer a more viable approach to the engineering of nanocrystalline diamond for electronic applications. This suggestion is generally applicable to nanodiamond particulates but also relates to nanocrystalline diamond thin films terminated (at the free surface) with {110} facets. The electronic properties of nanocrystalline diamond thin films are also affected by grain boundaries, which may differ in structure from a free surface.

Previous studies have used the DFTB method to examine the electronic properties of grain boundaries, and the approach used here is directly applicable. It was shown by Sternberg et al. that the electronic structure of a grain boundary is related to the density of atoms within the boundary layer, which of course is a direct result of the orientation of the terminal planes (facets) of the adjacent grains.[19] The {110} surface and a grain boundary containing one or more {110} planes both have a lower atomic density with 2-fold coordinated atoms, and both will readily hydrogenate given an available atomic hydrogen source.[20]

Conclusions

In conclusion, these DFTB simulations indicate that for small particles, within the quantum confinement regime, the band gap and Fermi energy of nanocrystalline diamond may be engineered using particle shape (as described by the type of terminal facets) as well as particle size. In reported DFT results it has also been found that the electronic properties depend on C−H bond length, as opposed to the specific location of terminating hydrogen atoms.[12] In the present study, the C−H bond length for all structures was fully optimized (in each case), but no statistically significant difference in the C−H bonds length could be discerned, and only complete passivation was examined. It is therefore likely that fine differences in electronic structure due to changes in the bonding configuration of passivation layers are only discernible from higher level simulations.

A systematic investigation of the relationship between electronic properties and the spatial distribution of inhomogeneous passivation layers is planned for the future, along with the investigation of the size and shape dependence of other properties such as work functions. In addition to this, based on the finding that the introduction of {110} facets may be instrumental in engineering the electronic structure, a complementary study is underway on alternative nanodiamond structures with varying degrees of {110} facet area and a more spherical appearance.

Acknowledgment. This project has been supported by the Australian Academy of Sciences under the J. G. Russell

Award and the Victorian Partnership Advanced Computing and the National Computing Infrastructure (NCI) national facility. I would like to thank Michael Sternberg from ANL for useful discussions throughout this project.

References

(1) Hu, Y.; Shenderova, O.; Hu, Z.; Padgett, C.; Brenner, D. *Rep. Prog. Phys.* **2006**, *69*, 1847.
(2) Danilenko, V. V. *Phys. Solid State* **2004**, *6*, 595.
(3) Sattel, S.; Robertson, J.; Tass, Z.; Scheib, M.; Wiescher, D.; Ehrhardt, H. *Diamond Relat. Mater.* **1997**, *6*, 255.
(4) Gruen, D. M. *Annu. Rev. Mater. Sci.* **1999**, *29*, 211.
(5) Raty, J.-Y.; Galli, G.; Bostedt, C.; Buuren, T. W.; Terminello, L. J. *Phys. Rev. Lett.* **2003**, *90*, 37402.
(6) Rutter, M. J.; Robertson, J. *Phys. Rev. B* **1998**, *57*, 9241.
(7) Drummond, N. D.; Williamson, A. J.; Needs, R. J.; Galli, G. *Phys. Rev. Lett.* **2005**, *95*, 096801.
(8) Geis, M. W.; Twichell, J. C.; Macaulay, J.; Okano, K. *Appl. Phys. Lett.* **1995**, *67*, 9.
(9) Breskin, A.; Chechik, R.; Shefer, E.; Bacon, D.; Avigal, Y.; Kalish, R.; Lifshitz, Y. *Appl. Phys. Lett.* **1997**, *70*, 3446.
(10) Raty, J. Y.; Galli, G. *J. Electro. Chem.* **2005**, *584*, 9.
(11) Wang, C.; Zheng, B.; Zheng, W. T.; Jiang, Q. *Diamond Relat. Mater.* **2008**, *17*, 204.
(12) Zhang, Z.; Dai, Y.; Huang, B. *Appl. Surf. Sci.* **2008**, *255*, 2623.
(13) Porezag, D.; Frauenheim, Th.; Kohler, Th.; Seifert, G.; Kaschner, R. *Phys. Rev. B* **1995**, *51*, 12947.
(14) Frauenheim, T.; Seifert, G.; Elstner, M.; Niehaus, T.; Kohler, C.; Amkreutz, M.; Sternberg, M.; Hajnal, Z.; Di Carlo, A.; Suhai, S. *J. Phys.: Condens. Matter* **2002**, *14*, 3015.
(15) Barnard, A. S.; Sternberg, M. *J. Mater. Chem.* **2007**, *17*, 4811. Barnard, A. S.; Sternberg, M. *J. Comput. Theor. Nanosci.* **2008**, *5*, 2089.
(16) Barnard, A. S. *J. Mater. Chem.* **2008**, *18*, 4038.
(17) Rezek, B.; Nebel, C. E. *Diamond Relat. Mater.* **2005**, *14*, 466.
(18) Takeuchi, D.; Ri, S.-G.; Kato, H.; Nebel, C. E.; Yamasaki, S. *Phys. Status Solidi A* **2005**, *202*, 2098.
(19) Sternberg, M.; Zapol, P.; Curtiss, L. A. *Phys. Rev. B* **2003**, *68*, 205330.
(20) Sternberg, M.; Kaukonen, M.; Nieminen, R. M.; Frauenheim, Th. *Phys. Rev. B* **2001**, *63*, 165414.